ORGANIC LETTERS

2011
Vol. 13, No. 17
4502–4505

[4]Pseudorotaxanes with Remarkable Self-Sorting Selectivities

Wei Jiang,[†,§] Dominik Sattler,[†] Kari Rissanen,[‡] and Christoph A. Schalley*[,†]

Institut für Chemie und Biochemie, Freie Universität Berlin, Takustrasse 3, 14195 Berlin, Germany, and Department of Chemistry, Nanoscience Center, University of Jyväskylä, P.O. Box 35, 40014 Jyväskylä, Finland

christoph@schalley-lab.de

Received June 16, 2011

ABSTRACT

The synthesis and characterization of several self-assembled [4]pseudorotaxanes is reported, some of which form in a programmed way based on two similar yet orthogonal crown ether/secondary ammonium ion binding motifs. A preference for the formation of a [4]pseudorotaxane with an antiparallel rather than parallel alignment of crown ether building blocks is observed even in the absence of such orthogonal binding sites, when a homodivalent axle is used.

Template effects,[1] self-assembly,[2] and self-sorting[3] are strategies to accomplish efficient supramolecular synthesis by programming simple building blocks constituting the final supramolecular architecture. One aim is to mimic natural and biological systems[4] and to go beyond that in the construction of functional synthetic complexes.[5] Intertwined molecules[6] such as (pseudo)rotaxanes have been intensely investigated in this respect. In order to expand the programmability of pseudorotaxane assemblies, we recently made use of the well-established crown/secondary ammonium ion template effect[7] by incorporating two orthogonal binding motifs in one building block.[8] For example, heterodivalent guest **1**-2H·2PF_6 and heterodivalent host **2** (Scheme 1a) self-sort into the [4]pseudorotaxane **3**-4H·4PF_6, while the 2:1:1 mixture of **1**-2H·2PF_6, **4**, and **5** gives rise to **6**-4H·4PF_6. The two crown ethers have different cavity sizes. Since the 21-crown-7 moiety is too narrow for the axle's central phenyl group to slip through,[9] the parallel or antiparallel arrangement of the axles can be

[†] Freie Universität Berlin.
[‡] University of Jyväskylä.
[§] Present address: The Scripps Research Institute, La Jolla, CA, USA.

(1) (a) Diederich, F.; Stang, P. J., Eds. *Templated Organic Synthesis*; Wiley-VCH: Weinheim, Germany, 2000. (b) Schalley, C. A.; Weilandt, T.; Brüggemann, J.; Vögtle, F. *Top. Curr. Chem.* **2004**, *248*, 141–200.

(2) (a) Lindsey, J. S. *New J. Chem.* **1991**, *15*, 153–180. (b) Whitesides, G. M.; Mathias, J. P.; Seto, C. T. *Science* **1991**, *254*, 1312–1319.

(3) (a) Mukhopadhyay, P.; Wu, A.; Isaacs, L. *J. Org. Chem.* **2004**, *69*, 6157–6164. (b) Wu, A.; Isaacs, L. *J. Am. Chem. Soc.* **2003**, *125*, 4831–4835. (c) Schmittel, M.; Mahata, K. *Chem. Commun.* **2010**, *46*, 4163–4165. (d) Rudzevich, Y.; Rudzevich, V.; Klautzsch, F.; Schalley, C. A.; Böhmer, V. *Angew. Chem., Int. Ed.* **2009**, *48*, 3867–3871.

(4) Lehn, J.-M. *Science* **2002**, *295*, 2400–2403.

(5) (a) Schalley, C. A.; Lützen, A.; Albrecht, M. *Chem.—Eur. J.* **2004**, *10*, 1072–1080. (b) Balzani, V.; Credi, A.; Raymo, F. M.; Stoddart, J. F. *Angew. Chem., Int. Ed.* **2000**, *39*, 3348–3391. (c) Collin, J.-P.; Dietrich-Buchecker, C.; Gaviña, P.; Jimenez-Molero, M. C.; Sauvage, J.-P. *Acc. Chem. Res.* **2001**, *34*, 477–487. (d) Amendola, V.; Fabbrizzi, L.; Mangano, C.; Pallavicini, P. *Acc. Chem. Res.* **2001**, *34*, 488–493.

(6) Sauvage, J.-P.; Dietrich-Buchecker, C. *Molecular Catenanes, Rotaxanes and Knots*; Wiley-VCH: Weinheim, 1999.

(7) (a) Clifford, T.; Abushamleh, A.; Busch, D. H. *Proc. Natl. Acad. Sci. U.S.A.* **2002**, *99*, 4830–4836. (b) Gibson, H. W.; Yamaguchi, N.; Hamilton, L.; Jones, J. W. *J. Am. Chem. Soc.* **2002**, *124*, 4653–4665. (c) Gibson, H. W.; Yamaguchi, N.; Jones, J. W. *J. Am. Chem. Soc.* **2003**, *125*, 3522–3533. (d) Badjić, J. D.; Ronconi, C. M.; Stoddart, J. F.; Balzani, V.; Silvi, S.; Credi, A. *J. Am. Chem. Soc.* **2006**, *128*, 1489–1499. (e) Northrop, B. H.; Aricó, F.; Tangchiavang, N.; Badjić, J. D.; Stoddart, J. F. *Org. Lett.* **2006**, *8*, 3899–3902. (f) Wong, W.-Y.; Leung, K. C.-F.; Stoddart, J. F. *Org. Biomol. Chem.* **2010**, *8*, 2332–2343. (g) Zhu, K.; Zhang, M.; Wang, F.; Li, N.; Li, S.; Huang, F. *New J. Chem.* **2008**, *32*, 1827–1830. (h) Wang, F.; Zheng, B.; Zhu, K.; Zhou, Q.; Zhai, C.; Li, S.; Li, N.; Huang, F. *Chem. Commun* **2009**, 4375–4377.

(8) (a) Jiang, W.; Schäfer, A.; Mohr, P. C.; Schalley, C. A. *J. Am. Chem. Soc.* **2010**, *132*, 2309–2320. (b) Jiang, W.; Schalley, C. A. *Proc. Natl. Acad. Sci. U.S.A.* **2009**, *106*, 10425–10429.

(9) (a) Jiang, W.; Winkler, H. D. F.; Schalley, C. A. *J. Am. Chem. Soc.* **2008**, *130*, 13852–13853. (b) Jiang, W.; Schalley, C. A. *Beilstein J. Org. Chem.* **2010**, *no. 14*, 6.

10.1021/ol201618f
Published on Web 07/28/2011

programmed into the building blocks. Similarly, an antiparallel arrangement of the crown heterodimers is realized in **3**-4H·4PF$_6$, while the two homodimers in **6**-4H·4PF$_6$ are threaded onto the axles in a sequence-controlled way. This integrative self-sorting based on orthogonal binding motifs incorporated in the key building blocks aims at the programmed construction of a more complex supramolecular architecture.

In the present contribution, we extend this concept to homodivalent axles **7**-2H·2PF$_6$ and **8**-2H·2PF$_6$ and their assemblies with crown ether heterodimer **2** (Scheme 1b). A 1:1:2 mixture of these components is expected to assemble into [4]pseudorotaxane **9**-4H·4PF$_6$, in which the two crown ether heterodimers are parallel to each other. With the help of ^{1}H,^{1}H COSY NMR spectra, the quite complex ^{1}H NMR spectra (Supporting Information) can be assigned and complexation-induced signal shifts typical for crown ether/ammonium ion complexes are observed. More straightforward evidence for the formation of **9**-4H·4PF$_6$ comes from tandem ESI mass spectrometry. The most intense peak at *m*/*z* 1422 in the ESI mass spectrum (Figure 1, top) of the 1:1:2 mixture in CH_2Cl_2 corresponds to doubly charged [**9**-4H·2PF$_6$]$^{2+}$. Peaks at *m*/*z* 1418 and 1426 correspond to the two singly charged 1:1 axle/crown ether complexes [**7**-2H·PF$_6$·**2**]$^+$ and [**8**-2H·PF$_6$·**2**]$^+$. They likely form during ionization by charge-repulsion-induced fragmentation. Further losses of HPF$_6$[10] then yield the ions at *m*/*z* 1272 and 1280. Thus, all signals in the mass spectrum can be traced back to [**9**-4H·2PF$_6$]$^{2+}$. No other assemblies have been observed; in particular, neither **10**-4H·4PF$_6$ nor **11**-4H·4PF$_6$ appear to point to a high self-sorting fidelity. The infrared multiphoton dissociation (IRMPD) experiments performed with mass-selected [**9**-4H·2PF$_6$]$^{2+}$ (Figure 1, bottom) clearly confirm the structure assignment. The [**9**-4H·2PF$_6$]$^{2+}$ dication fragments into two monocations at *m*/*z* 1426 and 1418 (Figure 1, right insets), which correspond to [**7**-2H·PF$_6$·**2**]$^+$ and [**8**-2H·PF$_6$·**2**]$^+$, respectively. This result is in agreement with expectation based on the closed structure of [**9**-4H·2PF$_6$]$^{2+}$: Charge separation is favorable, and in line with literature,[8b,10] a pseudosymmetric cleavage into two separate singly charged axle/crown fragments thus represents the least energy-demanding fragmentation pathway. The subsequent losses of neutral HPF$_6$ (or HF/PF$_5$) are also typical for such crown ether/secondary ammonium complexes. Therefore, the NMR, ESI-MS, and MS/MS results indicate that the [4]-pseudorotaxane **9**-4H·4PF$_6$ is the by far major assembly product in the 1:1:2 mixture of **7**-2H·2PF$_6$, **8**-2H·2PF$_6$, and **2**.

Scheme 1 [a]

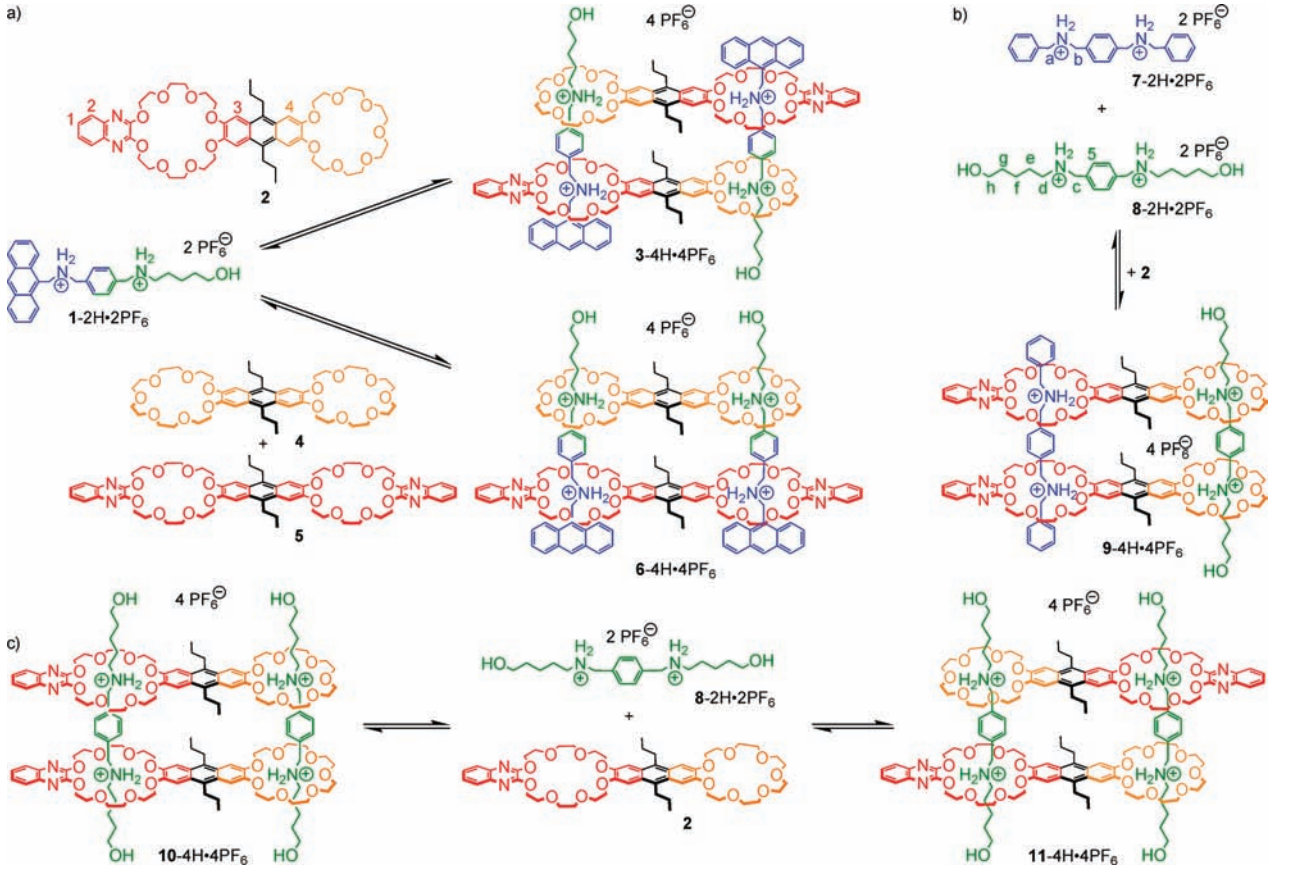

[a] (a) Self-assembly of [4]pseudorotaxanes **3**-4H·4PF$_6$ and **6**-4H·4PF$_6$ from heterodivalent axle **1**-2H·2PF$_6$ and crown ether dimers **2**, **4**, and **5** as reported earlier.[8] (b) Self-sorting of **9**-4H·4PF$_6$ from homodivalent axles **7**-2H·2PF$_6$, **8**-2H·2PF$_6$, and crown ether dimer **2**. (c) The equilibrium of **10**-4H·4PF$_6$ and **11**-4H·4PF$_6$ is shifted far to the antiparallel crown ether arrangement (> 49:1).

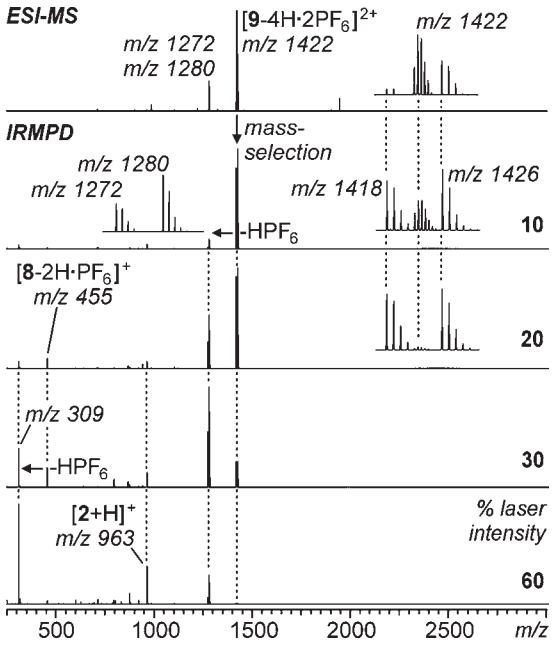

Figure 1. Top: ESI-FTICR mass spectrum of the 1:1:2 mixture of **7**-2H·2PF$_6$, **8**-2H·2PF$_6$, and **2** in CH_2Cl_2. Bottom: IRMPD experiments (MS/MS) of mass-selected [**9**-4H·2PF$_6$]$^{2+}$.

Hydroxypentyl-substituted ammonium ions are able to complex both crown ethers.[8,9] Therefore, axle **8**-2H·2PF$_6$ and wheel **2** (1:1) are expected to even form [4]pseudorotaxanes in the absence of **7**-2H·2PF$_6$. Two constitutional isomers may form: **10**-4H·4PF$_6$ with two parallel hosts and **11**-4H·4PF$_6$ with both crown dimers in an antiparallel arrangement. These two isomers have exactly the same binding motifs. Thus, no significant stability difference would be expected and both isomers should coexist in solution.The two isomers, however, have different symmetries. While **10**-4H·4PF$_6$ contains a mirror plane between the two crown ether dimers, a center of inversion exists in **11**-4H·4PF$_6$. Although both pseudorotaxanes have the same number of sets of NMR signals, the coupling patterns differ. In complex **10**-4H·4PF$_6$, two sets of signals for axle protons are expected, because both axles reside in different environments. Each of the axles bears two equivalent binding sites so that protons H-5 in the central axle phenyl group do not couple and two singlets should be observed, one for each of the axles. In pseudorotaxane **11**-4H·4PF$_6$, both axles are in identical environments, but each one has two nonequivalent binding sites. Therefore, the H-5 protons should couple yielding AA′XX′ systems.

The ^{1}H NMR spectrum (Figure 2c) of the 1:1 mixture of **8**-2H·2PF$_6$ and **2** exhibits only two sets of signals suggesting the predominance of only one isomer. Complexation-induced shifts relative to the signals of the two free components (Figure 2a,b) indicate the formation of the crown/ammonium complexes. In particular, protons H-3

(10) Jiang, W.; Schalley, C. A. *J. Mass Spectrom.* **2010**, *45*, 788–798.

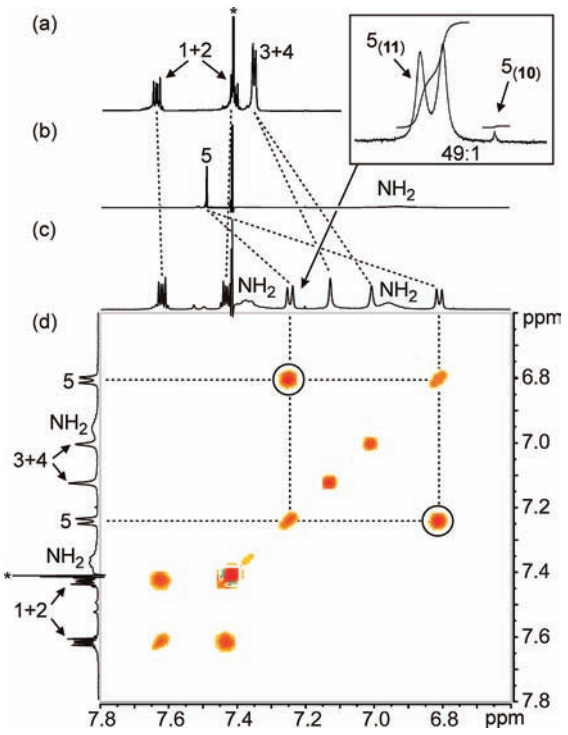

Figure 2. ^{1}H NMR spectra (500 MHz, 298 K, $CDCl_3/CD_3CN$ = 2:1, 2.0 mM) of (a) **2**, (b) **8**-2H·2PF$_6$, and (c) the equimolar mixture of **8**-2H·2PF$_6$ and **2**. Dotted lines indicate complexation-induced signal shifts of guest and host protons. (d) ^{1}H,^{1}H COSY spectrum (500 MHz, 298 K, $CDCl_3/CD_3CN$ = 2:1, 2.0 mM) of the equimolar mixture of **8**-2H·2PF$_6$ and **2**. Inset: Relative integration of signals for H-5 in **10**-4H·4PF$_6$ and **11**-4H·4PF$_6$. Numbers denote protons as assigned in Scheme 1. Asterisk = solvent residue ($CHCl_3$).

and H-4 of the central anthracene moiety and, most prominently, the H-5 protons experience upfield shifts. The ^{1}H,^{1}H COSY NMR spectrum helps to assign the H-5 protons to the two unresolved AA′XX′ systems at 7.25 and 6.81 ppm. The coupling between these two H-5 protons thus identifies **11**-4H·4PF$_6$ to be the by far predominant isomer in solution. Next to both of these AA′XX′ systems, i.e. at 7.20 and 6.76 ppm, two very small singlets appear, which we assign to H-5 of the **10**-4H·4PF$_6$ isomer. From the ≥49:1 integral ratio (Figure 2, inset), we obtain an equilibrium constant of $K \geq 49$ relating to a $\Delta\Delta G^{\circ} \geq 9.6$ kJ mol^{-1} between **10**-4H·4PF$_6$ and **11**-4H·4PF$_6$.

Figure 3 depicts the solid-state structure[11] of **11**-4H·4PF$_6$ which is in good agreement with the observed NMR shifts of the pseudorotaxane in solution. The axle phenyl groups are located within the plane of one anthracene and above the other anthracene spacer (plane-to-plane distance of 3.37 Å) thus experiencing the aromatic anisotropy and therefore, the corresponding NMR signals

(11) CCDC-829618. M = 2981.2, colorless prisms, 0.10 × 0.10 × 0.15 mm^3, monoclinic, space group $P2_1/n$, a = 14.1502(6) Å, b = 21.638(1) Å, c = 27.734(1) Å, β = 95.860(4)°, V = 8446.9(6) Å^3, Z = 2, D_c = 1.172 g/cm^3, T = 173(2) K, 917 parameters, R = 0.1646 [$I_o > 2\sigma(I_o)$], wR = 0.4406 (all reflections).

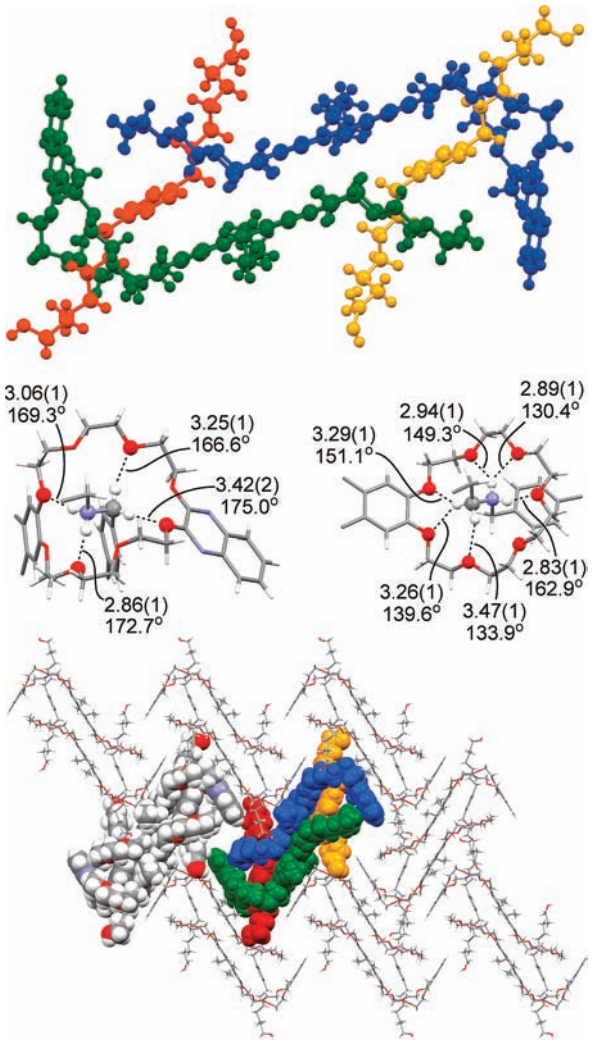

Figure 3. Crystal structure of **11**-4H·4PF$_6$. Top: Ball-and-stick representation with the pseudorotaxane components color-coded. Center: crown/ammonium binding motifs (left: 24-crown-8, right: 21-crown-7) with NH···O and CH···O hydrogen-bond lengths (A–B distances in Å) and angles (in degrees). Bottom: Packing pattern with two complexes in space-filling representation. The building blocks of the central complex are color-coded for clarity.

shift upfield. Also H-3 and H-4 shift upfield due to aromatic anisotropy of the two anthracenes, which are parallel but shifted sideways to each other. The crown-to-ammonium binding is mediated by N–H···O and C–H···O hydrogen bonds as indicated in Figure 3. In addition, aromatic stacking results in an attractive interaction between the two anthracenes, which are shifted against each other. The centrosymmetrical **11**-4H·4PF$_6$ complexes form loosely interacting rows which pack on top of each other with a half-a-molecule shift.

One of the reasons for the predominant formation of **11**-4H·4PF$_6$ is likely a favorable alignment of dipoles in the antiparallel arrangement of the two crown ether dimers. In addition, the two differently sized crown ethers also differ in rigidity, when the axle complexes to them. The 24-crown-8/ammonium complex is more flexible due to the larger cavity size. Both isomers, **10**-4H·4PF$_6$ and **11**-4H·4PF$_6$, therefore may well suffer from different geometric strain which accounts at least for part of the ca. 9.6 kJ mol^{-1} energy difference between them. Finally, the two quinoxaline heterocycles would be close to each other in **10**-4H·4PF$_6$, which might lead to an unfavorable arrangement of local dipoles.

In conclusion, the [4]pseudorotaxane architectures under study show interesting self-sorting properties based on orthogonal binding motifs as in **3**-4H·4PF$_6$,[8] **6**-4H·4PF$_6$, and **9**-4H·4PF$_6$. But even in the absence of orthogonal binding motifs, i.e. when only one axle, **8**-4H·4PF$_6$, is used, subtle effects lead to a precise control over the overall geometry of the complexes and **11**-4H·4PF$_6$ predominates over its isomer **10**-4H·4PF$_6$. Understanding these subtle effects will have a significant impact on our ability to program the outcome of self-assembly reactions and to construct the supramolecular architecture forming the basis of molecular devices.

Acknowledgment. We are grateful to the Deutsche Forschungsgemeinschaft (DFG; SFB 765 "multivalency"), the German Academic Exchange Service (DAAD), and the Academy of Finland (K.R., Project 212588 and 218325) for funding and thank Dr. N. Kodiah Beyeh (University of Jyväskylä) for fruitful discussions.

Supporting Information Available. Synthetic procedures, characterization data, crystallography details. This material is available free of charge via the Internet at http://pubs.acs.org.